1 **Cyclic AMP signalling and glucose metabolism mediate pH taxis by African trypanosomes**

2 Sebastian Shaw[1,2,#a], Sebastian Knüsel[1,♣], Daniel Abbühl[1,♣,#b], Arunasalam Naguleswaran[1,♣],
3 Ruth Etzensperger[1], Mattias Benninger[1] and Isabel Roditi[1,*]

4 [1] Institute of Cell Biology, University of Bern, Bern, Switzerland

5 [2] Graduate School of Cellular and Biomedical Sciences, University of Bern, Bern, Switzerland

6 ♣ These authors contributed equally

7 [#a] Current Address: Department of Pathobiology, School of Veterinary Medicine, University of
8 Pennsylvania, Philadelphia, PA 19104, USA

9 [#b] Current Address: Trypanosome Cell Biology Unit, INSERM U1201, Institute Pasteur, 75015
10 Paris, France

11 * Corresponding author

12 Email: isabel.roditi@izb.unibe.ch

13

Abstract

The collective movement of African trypanosomes on semi-solid surfaces, known as social motility, is presumed to be due to migration factors and repellents released by the parasites. Here we show that procyclic (insect midgut) forms acidify their environment as a consequence of glucose metabolism, generating pH gradients by diffusion. Early and late procyclic forms exhibit self-organising properties on agarose plates. While early procyclic forms are repelled by acid and migrate outwards, late procyclic forms remain at the inoculation site. Furthermore, trypanosomes respond to exogenously formed pH gradients, with both early and late procyclic forms being attracted to alkali. pH taxis is mediated by multiple cyclic AMP effectors: deletion of one copy of adenylate cyclase ACP5, or both copies of the cyclic AMP response protein CARP3, abrogates the response to acid, while deletion of phosphodiesterase PDEB1 completely abolishes pH taxis. The ability to sense pH is biologically relevant as trypanosomes experience large changes as they migrate through their tsetse host. Supporting this, a CARP3 null mutant is severely compromised in its ability to establish infections in flies. Based on these findings, we propose that the expanded family of adenylate cyclases in trypanosomes might govern other chemotactic responses in their two hosts.

33 **Introduction**

34 Environmental sensing, chemotaxis and quorum sensing present possibilities for pathogens to
35 orient themselves within their hosts. All three are widespread in bacteria, and the sensors and
36 response mechanisms have been characterised in detail[1,2]. Genes involved in bacterial
37 chemotaxis and quorum sensing have long been linked to biofilm formation and swarming
38 behaviour[3,4]. By contrast, very little is known about chemotaxis in unicellular eukaryotes, with
39 the exception of *Dictyostelium discoideum*, which generates and reacts to cyclic AMP (cAMP)
40 gradients, promoting aggregation and differentiation[5–8].

41 Intracellular pathogens frequently exploit receptor-ligand interactions to recognise and
42 invade the appropriate cell types[9–12]. For extracellular parasites such as *Trypanosoma brucei spp*.,
43 causative agents of human and animal trypanosomiasis, it is not known what drives them to
44 move from one host tissue to another. In their mammalian hosts, quorum sensing regulates the
45 titre of *T. brucei* by triggering the differentiation of proliferative slender forms to quiescent
46 stumpy forms[13,14]. When these are taken up by tsetse flies during a blood meal[15] they
47 differentiate to early procyclic (midgut) forms and then to late procyclic forms[16]. In addition to
48 the surface marker GPEET procyclin, which is only expressed by early procyclic forms, several
49 metabolic enzymes, nutrient transporters and signal transducers are differentially expressed
50 between the two forms[17,18]. Colonisation of the midgut by procyclic forms is followed by
51 additional rounds of differentiation as parasites invade the proventriculus, and then move to the
52 salivary glands before being transmitted to a new mammalian host. At present, however, the
53 cues allowing trypanosomes to orient themselves within their hosts are unknown.

54 Early procyclic forms engage in a form of group migration, known as social motility
55 (SoMo), when cultured on semi-solid surfaces such as agarose plates[18,19]. The parasites initially
56 remain at the inoculation site, dividing approximately once every 24 h, then the communities
57 start to form regularly spaced projections that extend by ~1 cm (500 body lengths) per day.
58 Communities on the same plate are able to sense each other and reorient to avoid contact
59 (Supplementary Video 1). Late procyclic forms do not exhibit SoMo, but they do produce a
60 repellent that is sensed by early procyclic forms[18]. Communities on plates also react to other
61 signals. Trypanosomes depleted of the spliced leader core protein SmD1 shed exosomes that act

62 as repellents[20], while bacterial colonies can act as attractants[21]. Various species of *Leishmania*,
63 parasites related to trypanosomes, respond chemotactically to a range of compounds including
64 amino acids, carbohydrates and sera, in liquid culture[22–25]. In none of these cases is it known
65 which genes mediate the responses.

66 Few genes have been implicated in SoMo. Concomitant depletion of adenylate cyclases
67 ACP1&2, or depletion of ACP6 on its own, resulted in a hyper-social phenotype (hyper-SoMo)
68 where the communities formed more projections and migrated more rapidly, suggesting that
69 these are negative regulators[26]. Interestingly, ACP1 and ACP6 are upregulated in late procyclic
70 forms[17], which are SoMo-negative[18]. The flagellar phosphodiesterase B1 (PDEB1)[19] and the
71 endoplasmic reticulum protein Rft1[27,28] are positive regulators of SoMo. Importantly, null
72 mutants of PDEB1 and Rft1 were not only impaired in SoMo, but also defective in colonising the
73 tsetse midgut[27,29]. We postulated that SoMo is largely a chemotactic response to factors
74 produced by the trypanosomes themselves. Here we show that procyclic forms can generate pH
75 gradients through glucose metabolism and that the response of early and late procyclic forms to
76 these gradients can explain the self-organising properties of communities on plates. In addition,
77 we identified two cAMP signalling components involved in the response to acid, ACP5 and the
78 cAMP response protein CARP3. Notably, pH sensing is completely abolished in PDEB1 knockout,
79 where cAMP levels are perturbed. pH taxis could be biologically relevant as there is a pH gradient
80 in the tissues that are colonised by the parasites during their transmission through the insect
81 host[30]. In support of this, we show that CARP3 null mutant parasites are severely compromised
82 in their ability to establish fly infections.

83 **Results**

84 **Parasite-secreted factors change properties of the medium and repel migrating projections**

85 What are the factors causing collective migration in SoMo? The fact that communities sense and
86 avoid each other over considerable distances means that they react to attractants or repellents
87 that are secreted, or otherwise released, by the parasites. We started by investigating if these
88 factors were produced under normal growth conditions in liquid culture. We concentrated the
89 supernatant of a dense culture (2×10^7 cells ml^{-1}) 10-fold and spotted this "conditioned medium"

90 (CM) next to migrating projections on SoMo plates (Fig. 1a, upper panel). Projections migrating
91 towards the site where CM was spotted reoriented away from it, indicating that it was perceived
92 as a repellent. In a second experiment, CM was either sterile filtered or dialysed (with a 12 kDa
93 cut-off) prior to concentration and spotted next to migrating projections. As seen with untreated
94 CM, filtered CM still repelled migrating projections (Fig. 1a, lower left panel), but dialysed CM
95 lost its repellent properties (Fig. 1a, lower right panel). On the contrary, migrating parasites were
96 attracted to dialysed CM in the same way that they were to concentrated fresh medium (DTM)
97 (Fig. 1a). These results suggested that repellents might be metabolites that were lost upon
98 dialysis.

99 **Trypanosomes acidify their environment in liquid culture and on agarose plates**

100 Trypanosomes secrete a variety of molecules that influence the pH of their environment[31,32].
101 Indicators for pH, such as phenol red, are commonly used for culture media and it is apparent
102 that dense cultures are more acidic than fresh medium or log phase cultures, as illustrated for
103 early procyclic forms growing in liquid culture (Fig. 1b). We therefore used a small tip micro glass
104 pH electrode to measure the pH in liquid culture and on agarose plates (Fig. 2). Fresh medium
105 has a pH of 7.46 ($\pm$ 0.02) and the supernatant of a log phase culture has a pH of 7.45 ($\pm$ 0.01) (Fig.
106 2a). The pH decreased to 6.95 ($\pm$ 0.00) when parasites were allowed to overgrow; this
107 corresponds to ~3-fold increase in the concentration of H^+ ions (Fig. 2a).

108 To measure the pH on plates, 2 x 10^5 parasites were inoculated either in the centre of a
109 plate (Fig. 2b, left row), or in pairs at a defined distance from each other (Fig. 2b, right row), and
110 the pH was measured after 2, 3 ,4 and 7 days post inoculation. We measured the pH in the centre
111 of a community, at the periphery of a plate and between two communities. The pH at the centres
112 of the communities decreased from 7.50 ($\pm$ 0.01) to 7.31 ($\pm$ 0.05) during the first three days and
113 decreased further to 6.96 ($\pm$ 0.05) between days 3 and 7 (Fig. 2b, c). The pH at the periphery also
114 started to decrease between day 3 and 7, possibly because of diffusion of H^+ ions from the
115 parasite communities. When communities were plated in pairs, the pH at the midpoint between
116 them also decreased over time (Fig. 2b, right row, arrow). Thus, communities acidify their vicinity
117 resulting in pH gradients on the plates.

118 We showed previously that trypanosomes needed to reach a threshold number before
119 they started migrating[18]. We now demonstrate that it is not the cell number *per se* that is critical,
120 but rather the need to establish a discernible pH gradient. When the same number of parasites
121 were inoculated onto plates containing different volumes of semi-solid medium, the time point
122 at which projections started to form was inversely proportional to the volume (Fig. 2d). This
123 would be consistent with larger volumes buffering the pH more effectively and requiring more
124 cells, and thus more time, before a gradient was established. We cannot exclude, however, that
125 other factors are also affected by the volume of the medium.

126 **Reaction of early and late procyclic forms to exposure to acid and alkali**

127 As a next step, we tested if manipulating the pH gradient had an influence on migration by
128 exposing early procyclic forms to external sources of acid or alkali (Fig. 3a, b). Early procyclic
129 forms were inoculated onto plates and incubated until the projections reached a length of about
130 2 cm. At this point, solutions of HCl or NaOH were pipetted onto the surface at a defined distance
131 (Fig. 3a) and the plates were incubated for 16-20 h. The migrating cells responded very strongly
132 to both solutions (Fig. 3b, Supplementary Videos 2 & 3). Exogenous NaOH acted as an attractant,
133 causing projections to reorient towards it (OH^- treatment), while HCl caused the projections to
134 stop moving outwards, or to move away from the acid (H^+ treatment). Using the same assay,
135 another 22 chemicals were tested (Supplementary Fig. 1). In most cases, when a solution was
136 acidic, the projections were repelled, and when a solution was basic, the cells were attracted to
137 it. These experiments also showed that the projections reacted to the pH rather than to specific
138 cations or anions in the solutions.

139 We next tested late procyclic forms since these do not perform SoMo. Late procyclic
140 forms did not respond to HCl (Fig. 3c, Supplementary Video 4), but they formed a limited number
141 of projections that migrated towards NaOH. Community lifts (Fig. 3c) confirmed that the
142 parasites were still GPEET-negative and had not dedifferentiated to early forms. In summary,
143 these results demonstrate that procyclic forms exhibit pH taxis, with alkali acting as an attractant
144 for both early and late procyclic forms. In contrast, there are stage-specific differences in their
145 reaction to acid.
146

147 **RNA-seq analyses suggest that SoMo is a response to self-generated gradients**

148 To better understand the mechanisms behind self-organisation of early and late procyclic forms,
149 and their pH responses, we performed RNA-seq under different conditions. A culture of procyclic
150 forms (>60 % GPEET-positive) was plated and allowed to form projections (Fig. 4a, far right). A
151 community lift with antibodies against procyclins showed that the tips were strongly positive for
152 GPEET, while the centre of the community stained more strongly for EP. Cells were isolated from
153 the tips and roots of projections (Fig. 4a, far right) and analysed by RNA-seq. Data confirmed that
154 markers of early procyclic forms were more highly expressed in the tips than the roots (Fig. 4a,
155 left; Supplementary Table 1a). Other transcripts that were more highly expressed in the tip were
156 not characteristic of early procyclic forms in liquid culture, such as cysteine-rich acidic integral
157 membrane protein (CRAM)[33], a microtubule-associated repetitive protein (MARP2)[34] and a
158 hypothetical protein (hypo; Tb927.9.10400). In addition, several adenylate cyclases were
159 differentially expressed on plates; ACP3 and ACP5 were ≥2-fold higher in the tip, while ACP6 and
160 another adenylate cyclase (GRESAG 4; Tb927.11.1480) were ≥2-fold higher in the root. The up-
161 regulation of high affinity glucose transporters (THT2 and 2A), glycolytic enzymes and
162 components of the glycosome (Fig. 4a, middle and Supplementary Table 1a) is suggestive of
163 higher glucose metabolism by the tip than the root. Increased expression of these transcripts is
164 also characteristic of early procyclic forms in liquid culture[17,18].

165 RNA-seq was also performed on the tips of communities exposed to acid or alkali (Fig. 4b
166 and Supplementary Table 1b). There were no significant differences (≥2-fold, p=0.05) between
167 non-exposed communities and those exposed to alkali. A single cation transporter (CatT,
168 Tb927.11.9000) was more highly expressed in cells exposed to acid, but the read counts were
169 extremely low in both cases. CatT and a copy of a contig (Tb11.v5.0514) were the only significant
170 differences in a comparison of acid- versus alkali-treated communities. Taken together, these
171 results suggest that self-generated pH gradients might be the normal driver of migration on SoMo
172 plates.

173

174

175

176 **Glucose contributes to the formation of pH gradients**

177 Since the RNA-seq data indicated that cells at the tip might metabolise glucose more actively
178 than cells at the root, we investigated the role of glucose in SoMo. For these experiments SDM80
179 medium was prepared with 1 mM glucose, 6 mM glucose or 6mM N-acetylglucosamine (GlcNAc),
180 which inhibits glucose uptake by binding to hexose transporters[35]. Early procyclic forms of Lister
181 427 Bern were inoculated onto plates and incubated for 6 days (Fig. 5a). The parasites in SDM80
182 with 1 mM glucose started migrating later than cells in SDM80 containing 6 mM glucose, and the
183 SoMo defect was even more pronounced when glucose uptake was blocked by GlcNAc. Under
184 these conditions the cells only formed rudimentary "knobs" at the edge of the community and
185 failed to form projections, even at later time points.

186 The reduced ability to migrate on plates can have a variety of causes, especially in the
187 context of glucose restriction. It might be due to longer population doubling times, motility
188 defects or inefficient energy metabolism. Procyclic cultures of Lister 427 Bern are stably GPEET-
189 positive[27,36]. Nevertheless, we assessed the proportion of early procyclic forms by flow cytometry
190 (Fig. 5b). Regardless of the medium in which the cells were grown, all cultures were ≥97 % GPEET-
191 positive. Furthermore, the glucose concentration had no impact on the population doubling time
192 (Fig. 5c) or intracellular ATP levels (Fig. 5d), both assessed in liquid culture. Previous work showed
193 that directional motility is important for SoMo and migration through the fly[29]. We therefore
194 assessed cell motility (Fig. 5e); no differences were observed between cells grown in the presence
195 or absence of glucose.

196 To investigate whether different glucose concentrations influence the culture pH, we
197 compared medium alone with liquid cultures of trypanosomes in log phase or high density (Fig.
198 5f). While the pH of log-phase cultures did not differ from that of medium alone, dense cultures
199 of parasites in SDM79 or SDM80 with 6 mM glucose strongly acidified the medium. The
200 concentration of H^+ in dense cultures, compared to log phase cultures, increased 2.53-fold
201 (±0.03) for SDM79 and 2.51-fold (±0.06) for SDM80 plus glucose. By contrast, cells grown in
202 SDM80 plus GlcNAc showed a smaller change in H^+ ion concentration (1.22-fold ±0.03). We next
203 measured pH changes for communities growing on plates (Fig. 5g). The ΔpH between the centre
204 and the periphery reached -0.31(± 0.02) for parasites on SDM79 and -0.37(± 0.02) for SDM80 +

205 6mM glucose, corresponding to a ≥2-fold difference in H^+ ions at the two locations, whereas
206 plates containing SDM80 + GlcNAc did not show a difference in pH. Taken together, these data
207 show that glucose is required for parasites to generate a pH gradient, and that this correlates
208 with their ability to perform SoMo.

209 **Cyclic AMP signalling is involved in the response to pH**

210 RNA-seq identified a number of differentially expressed transcripts, including that of the flagellar
211 pocket protein CRAM, which was more highly expressed in the tips than in the roots (Fig. 4a).
212 CRAM is not essential in procyclic culture forms[37]. When we generated knockouts, these grew at
213 the same rate as their parental line, but two out of three independent clones produced smaller
214 projections. Nevertheless, all three reacted to acid and alkali in the same way as wild-type cells
215 (Supplementary Fig. 2) so we did not proceed with additional analyses.

216 Several adenylate cyclases were also differentially expressed between the tip and the root
217 (Fig. 4a). Before we started analysing these and other members of the cAMP signalling pathway,
218 we tested whether PDEB1, which hydrolyses cAMP, had an influence on the pH response. When
219 the PDEB1 null mutant was exposed to alkali or acid, it showed no pH response (Fig. 6a). Notably,
220 the PDEB1 null mutant differs from both early procyclic forms, which react to acid and alkali, and
221 late procyclic forms, which form projections in response to alkali but do not respond to acid
222 (Supplementary Table 2).

223 Four cAMP response proteins (CARP1-CARP4) were previously identified in an RNAi
224 screen as mediating resistance to an inhibitor of PDEB1[38], but they have not been studied in the
225 context of SoMo. In our attempts to generate knockout cell lines for CARP 1 and 2, we only
226 obtained clones after single rounds of transfection. We did not pursue these further, however,
227 as the resistance genes were not integrated at the correct loci. We were able to obtain knockouts
228 of CARP3 and 4, however (Supplementary Fig. 3a). CARP4 null mutants did not show any
229 difference to the parental line when they were subjected to a standard SoMo assay
230 (Supplementary Fig. 3b) and were not analysed further. Deletion of CARP3, while not affecting
231 growth in liquid culture (Supplementary Fig. 3c) or on plates (Supplementary Fig. 4c and 4d), or
232 expression of the early marker GPEET (Supplementary Fig. 3d) resulted in a major SoMo defect

233 (Fig 6b, upper panel) reminiscent of the PDEB1 null mutant. The CARP3 knockout did not display
234 a motility defect in liquid culture (Supplementary Fig. 4a and b) and still reacted to alkali, but did
235 not react to acid on plates (Fig 6b, lower panel). An HA-tagged addback of CARP3, expressed
236 from a procyclin locus, partially rescued the SoMo phenotype (Fig 6b, upper panel), although the
237 projections were shorter than in the parental line. Importantly, the addback was now able to
238 sense and react to both acid and alkali (Fig 6b, lower panel).

239 We next assessed the requirement for CARP3 *in vivo*. For these experiments we generated
240 a null mutant in wild-type *T. b. brucei* Lister 427 using a recently described CRISPR/Cas9 transient
241 expression system[39]. In addition, we engineered an addback ectopically expressing an untagged
242 version of CARP3 (Supplementary Fig. 5). Flies were infected with either the wild type, the
243 knockout or the addback and evaluated for the prevalence and intensity of midgut infections
244 after 14 days. The knockout showed a significantly lower midgut infection rate ($p < 0.00001$,
245 Fisher's exact test, two-sided) when compared to the wild type. In addition, infection intensities
246 were reduced (Fig 6c). Both the prevalence and intensities of infection with the addback were
247 comparable to the wild type. Thus, the defect in establishing a midgut infection can be attributed
248 specifically to the loss of CARP3. In addition, whereas 55-60% of flies heavily infected with the
249 wild type, and 100% heavily infected with the addback, had trypanosomes in the proventriculus,
250 the knockout gave no heavy midgut infections nor did it colonise the proventriculus
251 (Supplementary Table 3).

252 CARP3 is present in both the cytoplasm and the flagellum (Supplementary Fig. 4e;
253 www.tryptag.org). Since no interaction partners have been reported, a pulldown was performed
254 with HA-tagged CARP3 (Fig. 6d) and analysed by mass spectrometry. This led to the identification
255 of adenylate cyclases ACP3 and ACP5 in two biological replicates (Supplementary Table 4). These
256 interactions were confirmed by *in situ* tagging and co-immunoprecipitation of myc-tagged
257 versions of ACP3 and ACP5 in the CARP3-HA addback line (Fig. 6d and Supplementary Table 4).
258 The reciprocal co-immunoprecipitations with anti-myc antibody confirmed the interaction for
259 both ACP3 and ACP5 (Fig. 6d and Supplementary Table 2). These results, combined with their
260 differential expression in the tips and roots of projections (Fig. 4a) stimulated us to revisit some
261 of the flagellar ACP previously characterised by Lopez and coworkers[26]. In their study they

262 showed that knockdown of ACP1/2 or ACP6 by RNAi resulted in a hyper-SoMo phenotype. We
263 obtained null mutants of ACP2 and ACP6, but it was only possible to generate single knockouts
264 of ACP1 and ACP5 (Supplementary Fig. 6a) implying that they are essential at this stage of the life
265 cycle. Although we attempted to knock out ACP3, and isolated resistant cell lines, the antibiotic
266 resistance genes were not integrated at the correct locus (data not shown). The full knockout of
267 ACP6 and the semi-knockout of ACP1 both exhibited hyper-SoMo phenotypes, while the full
268 knockout of ACP2 showed no phenotype (Supplementary Fig. 6b). These results are consistent
269 with the findings with the RNAi lines; they also indicate that the hyper-SoMo phenotype in the
270 previously published ACP1/2 RNAi line[26] was due to depletion of ACP1. Unexpectedly, however,
271 and in contrast to the results with RNAi[26], single knockouts of ACP5 were unable to form
272 projections on plates (Fig. 6e, upper panel). In terms of their pH response, ACP5 single knockouts
273 resembled CARP3 double knockouts - they were able to form projections migrating towards an
274 alkaline source, but were refractory to acid (Fig. 6e, lower panel). Further experiments showed
275 that >80 % of these cells were GPEET-positive and that the phenotype of the ACP5 mutants was
276 not due to defects in growth or motility (Supplementary Fig. 6c-6f). These experiments also
277 revealed that ACP5-myc was localised exclusively at the flagellar tip (Fig 6f). In summary, we have
278 extended the catalogue of cAMP signalling components that are involved in regulating SoMo. In
279 addition, the finding that PDEB1, ACP5 and CARP3 play a role in the perception of environmental
280 acidity/alkalinity is consistent with SoMo being a response to self-generated pH gradients.

281 **Discussion**

282 It was proposed more than a decade ago that the collective migration of trypanosomes on plates
283 could be explained by a combination of migration factors and repellents released by the
284 parasites[19], but the identity of these molecules was unknown. Here we show for the first time
285 that trypanosomes acidify their environment as a consequence of glucose metabolism,
286 generating pH gradients by diffusion. While it is commonly assumed that free glucose levels in
287 tsetse are low between blood meals, and this is often stated in reviews, there are no primary
288 publications on this topic. The fact that transcripts encoding high affinity glucose transporters
289 and glycolytic enzymes are not only upregulated in SoMo tips (Figure 4) and in early procyclic

290 forms[17], but also in trypanosomes at the beginning of a fly infection[40], is compatible with procyclic
291 forms utilising carbon sources other than proline in tsetse.

292 Early and late procyclic forms exhibit self-organising properties. It is the perception of
293 these self-generated pH gradients that governs the outward migration of early procyclic forms
294 towards a more alkaline environment, while late procyclic forms remain at the inoculation site.
295 Local acidification of the environment, and the response to it, can also explain the spacing
296 between projections emanating from the same parasite colony, as well as the cessation of
297 migration or the reorientation of projections from two separate communities on the same plate.
298 In addition, it explains why the start of migration is not solely dependent on a threshold cell
299 number, as was previously reported[18], but rather on the external pH. Early procyclic forms are
300 also able to perceive exogenous sources of acid and alkali as repellents and attractants,
301 respectively. Late procyclic forms are also attracted to a more basic environment, but unlike early
302 procyclic forms they are not repelled by acid, explaining why they remain at the inoculation site
303 on plates and do not perform SoMo.

304 Analyses of the transcriptomes of cells spontaneously performing SoMo, or reacting to
305 exogenous alkali or acid, are consistent with them being the same response. Comparison of the
306 transcriptomes of trypanosomes at the tips and roots of projections showed that migrating cells
307 at the tip expressed high levels of markers for early procyclic forms. This mirrors what is seen in
308 liquid culture[17,18] as well as at early time points after flies are infected with stumpy forms[40].
309 Among the adenylate cyclases differentially expressed between the tip and the root, ACP6 is
310 more highly expressed at the root and is also up-regulated in late procyclic forms. By contrast,
311 ACP3 and ACP5, which are more highly expressed in the tip, are not stage-regulated between
312 early and late procyclic forms in liquid culture[17]. This is also true of a few other transcripts, such
313 as CRAM, and may reflect a response to culture on plates.

314 cAMP signalling is required for the perception of pH gradients (summarised in Fig. 6g). A
315 PDEB1 knockout was not only defective in SoMo[29], but was also impervious to acid and alkali. In
316 contrast to an RNAi mutant of ACP5 which still performed SoMo normally[26], an ACP5 single
317 knockout did not form projections and was insensitive to exogenous acid, but was still attracted
318 to alkali. In this respect, its behaviour resembles that of late procyclic forms. Down-regulation or

319 deletion of ACP6 ([26] and Supplementary Fig. 6b) or deletion of one copy of ACP1 cause hyper-
320 SoMo, while ACP2 is not required for SoMo or pH taxis. ACP1, ACP5 and ACP6 are localised at the
321 flagellar tip ([41] and Fig. 6f), highlighting its importance as a sensor.

322 For the first time, we show that there is a physical link between a cyclic AMP response
323 protein, CARP3, and adenylate cyclases ACP3 and ACP5. Moreover, the CARP3 null mutant had
324 the same defects in SoMo and acid sensing as the ACP5 single knockout. Interestingly, there is
325 strong evidence that CARP3 is N-myristoylated[42], which could enable it to associate with the inner
326 leaflet of the plasma membrane. N-myristoylation has been shown to regulate signalling in
327 mammals[43] and it is conceivable that acylated and non-acylated forms of CARP3 enable signals
328 to be transmitted from the membrane to the interior of the cell. *T. brucei*, which has the most
329 complex life cycle of all the African trypanosomes, also encodes the largest number of adenylate
330 cyclases. Many of these are stage-regulated, and it is plausible that they have functions in
331 reacting to their local environment. It is also worth noting that CARP3 interacts with other
332 adenylate cyclases, although ACP3 and ACP5 were the top hits (Supplementary Table 4), and that
333 it was recently identified by proximity labelling as interacting with ACP1[44].

334 pH taxis by trypanosomes is likely to be biologically relevant during fly transmission as
335 there are large differences between the pH of the midgut (pH ~8) and proventriculus (pH ~10.5)[30].
336 This would enable parasites to follow cues provided by the fly as they migrate to different
337 compartments. The hindgut is also more basic than the posterior midgut[30], and trypanosomes
338 have been detected there, but these have abnormal morphologies[45]. At present we do not know
339 if there are additional chemotactic cues attracting trypanosomes towards to the proventriculus
340 or repelling them from the hindgut. Regardless of whether they migrate in one or both directions,
341 only parasites migrating to the proventriculus can survive and complete the life cycle. We have
342 shown that CARP3 is required for efficient colonisation of tsetse. Interestingly, the knockout has
343 a more severe phenotype than the PDEB1 knockout described previously[29]. The finding that
344 CARP3 interacts with several adenylate cyclases in addition to ACP3 and 5 suggests that it may
345 act as a node for signal perception via cAMP signalling. It is established that procyclic forms
346 respond chemotactically to other effectors[20,21], but their identities are unknown. Chemotaxis
347 may also explain how parasites in the mammalian host disperse from the bloodstream into other

348 tissues [46–48]. Finally, the concept that self-generated gradients help drive directionality and speed
349 expansion into new territories, recently described for bacteria[49], may also apply to
350 trypanosomes.

351 **Methods**

352 **Trypanosome stocks and culture conditions**

353 Procyclic forms of EATRO1125 were derived from bloodstream forms of *T. b. brucei* AnTat1.1[50].
354 Early procyclic forms were cultivated at 27 °C and 2.5 % CO_2 in DTM supplemented with 15 %
355 foetal bovine serum (FBS) [51]. Late procyclic forms were cultured in SDM79[52] containing 10 % FBS
356 at 27 °C. Parasites were maintained at a density between 10^6 and 10^7 cells ml^{-1}. Procyclic forms
357 of *T. b. brucei* Lister 427 and derivatives thereof were cultured in SDM79 or SDM80 containing
358 10 % FBS at 27 °C. SDM80 components were as described[53], except that BME vitamin solution
359 100x (Bioconcept 5-20K00-H) was used instead of vitamin mix 100x (Invitrogen 010144) and 1%
360 Pen/Strep stock solution (Bioconcept 4-01F00-H) was used instead of 0.1 mM kanamycin.
361 Glucose-free SDM80 medium was supplemented with 10 % FBS, which results in a final
362 concentration of ~1 mM glucose. If indicated, SDM80 + 10 % FBS was supplemented with 6 mM
363 D-glucose or 6 mM N-Acetyl-D-glucosamine (GlcNAc) from a 1.2 M stock solution in water.
364 Population doubling times were determined over a period of at least 5 days in which the cell
365 density was determined daily.
366

367 **SoMo assays and community lifts**

368 The protocol to produce plates was adapted from Imhof and coworkers[18]. Plates were always
369 used on the same day that they were poured. Culture medium (10 ml) supplemented with 0.4 %
370 agarose (Promega V3125) was poured into petri dishes (85 mm diameter). Open plates were then
371 air-dried for 1 hour in a laminar flow hood. Cells from an exponentially growing culture were
372 centrifuged briefly and resuspended in the residual medium at a density of 4 x 10^7 cells ml^{-1}. Two
373 hundred thousand cells were spotted per inoculum; plates were sealed with parafilm and

374 incubated in a humidified environment at 27 °C and 2.5 % CO_2. Photographs of plates were taken
375 using a Nikon E8400 camera.
376 Community lifts for the detection of GPEET and EP procyclins were performed as
377 described[18], using nitrocellulose filters (Whatman Protran BA85), K1 rabbit anti-GPEET[36] at a
378 dilution of 1:1000 and TBRP1/247 mouse anti-EP (Cat. no. CLP001A, Cedarlane Laboratories,
379 Burlington, Canada) at a dilution of 1:2500 as primary antibodies (1 h incubation time at room
380 temperature). The secondary antibodies goat anti-mouse IRDye 800CW (LI-COR Biosciences, Bad
381 Homburg, Germany) and goat anti-rabbit IRDye 680LT (LI-COR Biosciences) were used at dilutions
382 of 1:10000 (1 h incubation time at room temperature). The filters were rinsed 3 times in TBS +
383 0.05 % Tween (Sigma), followed by one final rinse in PBS before being dried overnight at room
384 temperature and scanned on a LI-COR Odyssey Infrared Imager model 9120, using Odyssey
385 Application Software, Version 3.0.21.

386 **pH measurements on SoMo plates and in liquid cultures**

387 To monitor pH changes in liquid culture and on agarose plates, trypanosomes were cultured in a
388 humidified incubator at 27 °C and 2.5 % CO_2. SoMo plates were kept in the same incubator,
389 without sealing the lids with parafilm. For analysis of growth rate and pH measurements, cells
390 were maintained between 1 – 10 x 10^6 cells ml^{-1} by daily monitoring and dilution. "Log-phase"
391 samples had densities of 3 – 9 x 10^6 cells ml^{-1}. If not stated otherwise, "dense" samples were
392 obtained from cultures with a concentration of 1 - 1.5 x 10^7 cells ml^{-1} without further dilution for
393 2 days. "Medium only" refers to complete medium incubated in a culture flask in a humidified
394 incubator at 27 °C and 2.5 % CO_2 for at least 12 h. The pH of culture supernatants or SoMo plates
395 was measured using a micro electrode (Thermo Scientific™ Orion™ 9810BN Micro pH Electrode;
396 fisher scientific).

397 **Preparation of concentrated supernatant**

398 Early procyclic forms were grown until they reached a concentration of 3 x 10^7 cells ml^{-1}. The cells
399 were centrifuged for 5 minutes at 2500 g and the conditioned medium was transferred to a new
400 tube. Conditioned medium was either concentrated directly or first sterile filtered (Jet Biofil
401 syringe filter, 0.22 µm, REF: FVP203030K) or dialysed. 2 ml of conditioned medium were dialysed

402 with dialysis tubing cellulose membranes (Sigma-Aldrich, cut-off 12 kDa, REF: D9777-100FT)
403 against 50 ml DTM supplemented with 15 % FBS at 4 °C in two rounds (16 hours, then 12 hours).
404 To concentrate the conditioned medium, 1 ml was transferred into a 1.5 ml Eppendorf tube and
405 vacuum centrifuged for several hours until 100 µl remained in the tube. As a control, DTM only
406 was concentrated in parallel.

407 **pH taxis assay**

408 Procyclic forms were inoculated onto plates as described for SoMo assays. Following incubation
409 at 27 °C for four days, concentrates of 30 µl conditioned medium or medium only, or different
410 chemical solutions were added to the plates at a distance of 1.5 cm from migrating projections
411 (Fig. 3a, D = distance). The plates were sealed with parafilm and incubated at 27 °C for 16-20
412 hours. Stock solutions were prepared at a concentration of 1M, if not stated otherwise.

413 **Hot phenol extraction of RNA from migrating tips**

414 Plates containing semi-solid DTM medium were inoculated with 2 x 10^5 cells from a culture of
415 procyclic form EATRO1125 (60 – 80 % GPEET-positive). Following incubation for 6 – 7 days, tip
416 and root samples were collected from projections that were ≥2.5 cm long. For collecting tips
417 reacting to acid or alkali, 3 x 10^5 cells were seeded, incubated for five days and then 30 µl 1M
418 NaOH or 1M HCl were added on two sides of migrating cells at a distance of 1.5 cm from the tips
419 (Fig. 3a, D = distance). In total, between 70-100 tips of migrating projections, that were exposed
420 to acidic or alkaline solutions for 16 hours, were harvested. Only tips that clearly showed a
421 reaction were collected (usually 5-7 tips per community).
422 Cells were harvested by punching out a piece of agarose using an inverted P2 micro tip
423 (outer and inner diameters 6 and 4.5 mm, respectively). The tip subpopulation refers to the
424 outermost 3 mm of protrusions. The root refers to the region at the base of the projection as
425 shown in Figure 4a. Between 20-25 tips or 3-5 root samples were transferred into 1 ml DTM in a
426 24-well plate well. Cells were washed off the agarose pieces by careful rinsing with a P1000
427 pipette and the cell suspension was transferred to a 1.5 ml Eppendorf tube. The agarose pieces
428 were rinsed once more with 0.5 ml DTM, added to the cell suspension and centrifuged for 2
429 minutes at 3300 x g. On average, approximately 1 x 10^5 cells were retrieved from each tip and 6

430 x 10^5 cells from each root sample. For tips reacting to acid or alkali, the wells of a 6-well plate
431 contained a larger number of samples (up to 100 tips). In this case, the supernatant was carefully
432 aspirated from the well and collected in a 15 ml Falcon tube and the agarose pieces were washed
433 twice with 4 ml medium. The washes were added to the cells in the 15 ml Falcon tube and
434 centrifuged for 5 minutes at 2500 g. Cell pellets were resuspended in 50 µl residual medium and
435 RNA was extracted with hot phenol as described[54].

436 **RNA-seq analysis**

437 Total RNA (maximum 10 µg) was processed and used for Illumina sequencing as described
438 previously[17]. Poly(A)-selected RNAs were used for the preparation of cDNA libraries using an
439 Illumina TruSeq kit. Sequencing of cDNA libraries was performed at Fasteris, Geneva, using
440 Illumina HiSeq sequencing systems with 150 bp read lengths and sequencing depths of
441 approximately 20 million reads per sample. Reads were mapped to the *T. b. brucei* 927 reference
442 genome version 5.1, using the bowtie2 tool available in the Galaxy Interface (usegalaxy.org) with
443 default parameters that allow a maximum of 2 mismatches per 28 bp seed (Galaxy version
444 1.1.2). Read counts were extracted using "featureCounts" tool available in Galaxy using
445 TritrypDB-41 GFF annotation file. DESeq2 analysis were performed to identify the differentially
446 regulated genes and RPM values were calculated to estimate the transcripts abundance. Raw
447 read files are deposited at the European Nucleotide Archives (ENA) http://www.ebi.ac.uk/ena as
448 study PRJEB41935.

449 **Flow cytometry**

450 Cells were fixed in 2 % (w/v) PFA/PBS at 4°C overnight at a concentration of 1 x 10^7 cells ml^{-1} and
451 processed for flow cytometric analysis as previously described[55,56]. Rabbit antiserum α-GPEET
452 K1[36] and Alexa Fluor 488-conjugated secondary antibody (Invitrogen, Thermo Fisher Scientific)
453 were used at 1:1000 dilution in 2 % BSA/PBS and incubated for 1.5 h at 4 °C with rotation. To
454 remove particles of subcellular size, a cut-off of 7.5 x 10^5 was applied to the forward scatter. A
455 total of ten thousand events were recorded using a ACEA NovoCyte flow cytometer and analysed
456 without gating using FlowJo software version 10.6.1 (BD Life Sciences).

457 **Determination of steady-state ATP levels**

458 ATP concentrations were measured based on a previously described ATP production assay[57]. To
459 measure steady-state ATP levels in whole cells, cells were washed twice in ice-cold PBS and
460 resuspended in PBS at 2.5 x 10^7 cells ml^{-1}. Denaturation with perchloric acid, precipitation and
461 neutralisation with KOH was performed as described[57]. The cleared lysate was serially diluted 4-
462 fold in H_2O. Routinely, cells were harvested in triplicate and the second dilution of the cleared
463 lysate (16-fold dilution) was used for the bioluminescence assay. For each replicate, ATP
464 concentrations were measured in triplicate. ATP concentrations were determined using the ATP
465 Bioluminescence Assay Kit CLS II (Roche 11699695001, from Sigma-Aldrich) according to
466 manufacturer's instructions. For each dilution, 10 µl was added to 40 µl of 0.5 M Tris-acetate, pH
467 7.75 and supplemented with luciferase reagent to a final volume of 100 µl. Titrations of the ATP
468 standard supplied were analysed in parallel. Luminescence was measured in 96-well microtitre
469 plates (opaque, non-binding) using a Turner BioSystems Modulus Microplate Luminometer,
470 Model 9300-001. Signals were integrated over 5 sec in steady-glo mode. Three readings per plate
471 were acquired, with a period of 10 min. Values of the second reading were used for analysis,
472 since only the second and third readings yielded stable signals.

473 **Motility assays**

474 Cultures were allowed to grow to a density between 4 - 7 x 10^6 cells ml^{-1} and adjusted to a final
475 concentration of 5 x 10^6 prior to the experiment. These cells (in medium) were placed into
476 motility chambers[58]. To prevent cell adherence, the chamber was precoated with 1 % poly L-
477 glutamic acid (Fisher Scientific, P4886-25MG) for one hour and washed twice with 70 % EtOH.
478 The chambers were then washed twice with 100 µl medium and once with cell suspension before
479 loading 100 µl of cells at a concentration of 5 x 10^6 cells ml^{-1}. The edges of the coverslip were
480 sealed to avoid evaporation and capillary flow of liquid. Time lapse movies were recorded at 200
481 ms, with 250 cycles and 10 x magnification with a Leica DM 5500B microscope. The dataset was
482 analysed with a tracking macro provided by Richard Wheeler, University of Oxford[59]. Velocity,
483 speed and individual cell tracks were plotted using Fiji version 1.0[60] and Prism Version 6.
484

485 **Immunoprecipitation and proteomic analysis**

486 Isolation of HA-tagged protein complexes was performed as previously described[61] using the
487 addback cell line expressing CARP3-HA, or derivatives expressing CARP3-HA and either ACP3-myc
488 or ACP5-myc. Myc-tagged proteins were immunoprecipitated with 5 µg monoclonal antibody
489 9E10 (Cat No: MA1-980) and Dynabeads™ Pan Mouse IgG (Cat No: 11041), both from
490 ThermoFisher Scientific (Invitrogen). Isolated protein complexes were subjected to Western blot
491 analysis, or protein bands were cut from Coomassie-stained polyacrylamide gels, subjected to
492 trypsin digestion and proteins were identified by LC-tandem mass spectometry[62] at the
493 Proteomics and Mass Spectrometry Core Facility of the University of Bern.

494 **Generation of knockouts and addbacks**

495 Single knockouts, double knockouts and tagged addbacks used for all *in vitro* experiments were
496 generated in the parental 427 Cas9 cell line[29]. The CARP3 double knockout used for fly
497 experiments was generated in *T. b. brucei* Lister 427[36] using transiently expressed Cas9 and T7
498 RNA polymerase[39]. An addback ectopically expressing CARP3 was derived from the null mutant.
499 Targeting cassettes were amplified from pPOTv7-hygromycin and pPOTv7-G418[63] plasmids. The
500 primers used for PCR amplification of the targeting fragments and the sgRNA templates were
501 designed using LeishGEdit. These primers and the primers used for genotyping PCRs can be found
502 in Supplementary Table 5. The knockouts and the addback were verified by PCR (Supplementary
503 Table 5). To generate addbacks, HA-tagged and untagged versions of CARP3 were cloned into the
504 pGAPRONE-ΔLII[64] derivate pG-mcs-puro[65], linearised with Spe I and integrated upstream of a
505 procyclin locus on chromosome 6. Transfection was performed as described previously[66] using
506 TbBSF transfection buffer[67]. Stable transformants were selected using 15 µg ml^{-1} Geneticin G418
507 sulphate, 25 µg ml^{-1} hygromycin and 1 µg ml^{-1} puromycin.

508 **Immunofluorescence analysis (IFA) of HA- and or Myc-tagged cells**

509 Cells were harvested at a density of 2 – 5 x 10^6 cells and then washed once with PBS. They were
510 left to settle on a coverslip for 20 minutes and then fixed with 4 % PFA in PBS for 4 minutes. After
511 removing the supernatant, the cells were permeabilized with Triton-x 100 diluted to 0.2 % in PBS

512 for 5 minutes and the liquid was aspirated. The samples were blocked in PBS + 4 % BSA for 1 hour
513 at RT. The primary antibodies (monoclonal α-HA rat 3F10 and monoclonal α-myc mouse 9E10,
514 from Roche, distributed by Sigma Aldrich) were diluted 1:1000 and 1:500 respectively in PBS +
515 0.4 % BSA and the samples incubated for 1 hour at RT. The cells were then washed 3 times with
516 PBS and the supernatant aspirated after every washing step. They were then incubated with the
517 secondary antibodies AlexaFluor 488 conjugated donkey α-rat (Life Technologies) and AlexaFluor
518 488 conjugated goat α-mouse (Invitrogen/Thermo Fisher) both diluted 1:2000 in PBS + 0.4 % BSA
519 for 1 hour at RT. The samples were then washed 3 times as described for the primary antibodies
520 and incubated with Hoechst 33342 (20µg/ml) diluted 1:500 in PBS for 2 minutes. After three
521 washing steps, the cover slips were mounted on microscope slides with Mowiol and imaged with
522 a Leica DM 5500B microscope with a 100x objective. The acquired images were processed with
523 Fiji[60].

524 **Fly infections**

525 *Glossina morsitans morsitans* pupae were purchased from the Department of Entomology,
526 Slovak Academy of Science, Bratislava, Slovakia or were a kind gift from Jan van den Abbeele,
527 Institute of Tropical Medicine, Antwerp, Belgium. Teneral flies were infected by membrane
528 feeding with 2.5×10^6 parasites ml^{-1} and maintained on horse blood as described[36], except that
529 pupae and flies were kept at 24°C, 65 -70 % humidity, rather than 27 °C in the original protocol.
530 Flies were dissected and midgut infections were analysed on days 13 and 14 post infection. The
531 intensities of infections were graded as described[36].

532

533

534 **References**

535 1. Aframian, N. & Eldar, A. A Bacterial Tower of Babel: Quorum-Sensing Signaling Diversity
536 and Its Evolution. *Annu. Rev. Microbiol.* **74**, 587–606 (2020).
537 2. Yang, W. & Briegel, A. Diversity of Bacterial Chemosensory Arrays. *Trends Microbiol.* **28**,
538 68–80 (2020).
539 3. Daniels, R., Vanderleyden, J. & Michiels, J. Quorum sensing and swarming migration in
540 bacteria. *FEMS Microbiol. Rev.* **28**, 261–289 (2004).
541 4. Burkart, M., Toguchi, A. & Harshey, R. M. The chemotaxis system, but not chemotaxis, is
542 essential for swarming motility in *Escherichia coli*. *Proc. Natl. Acad. Sci. U. S. A.* **95**, 2568–
543 2573 (1998).
544 5. Tyson, J. J. & Murray, J. D. Cyclic AMP waves during aggregation of *Dictyostelium*
545 amoebae. *Development* **106**, 421–426 (1989).
546 6. Tomchik, K. J. & Devreotes, P. N. Adenosine 3',5'-monophosphate waves in *Dictyostelium*
547 *discoideum*: a demonstration by isotope dilution--fluorography. *Science* **212**, 443–446
548 (1981).
549 7. Maeda, M. *et al.* Periodic signaling controlled by an oscillatory circuit that includes
550 protein kinases ERK2 and PKA. *Science* **304**, 875–878 (2004).
551 8. Wang, M., Aerts, R. J., Spek, W. & Schaap, P. Cell cycle phase in *Dictyostelium discoideum*
552 is correlated with the expression of cyclic AMP production, detection, and degradation.
553 Involvement of cyclic AMP signaling in cell sorting. *Dev. Biol.* **125**, 410–416 (1988).
554 9. Kahn, S. *et al. Trypanosoma cruzi* amastigote adhesion to macrophages is facilitated by
555 the mannose receptor. *J. Exp. Med.* **182**, 1243–1258 (1995).
556 10. Kanjee, U. *et al. Plasmodium vivax* strains use alternative pathways for invasion. *J. Infect.*
557 *Dis.* (2020) doi:10.1093/infdis/jiaa592.
558 11. Kedzierski, L. *et al.* A leucine-rich repeat motif of *Leishmania* parasite surface antigen 2
559 binds to macrophages through the complement receptor 3. *J. Immunol.* **172**, 4902–4906
560 (2004).
561 12. Xing, M. *et al.* A Sialic Acid-Binding Protein SABP1 of *Toxoplasma gondii* Mediates Host
562 Cell Attachment and Invasion. *J. Infect. Dis.* **222**, 126–135 (2020).

563 13. Reuner, B., Vassella, E., Yutzy, B. & Boshart, M. Cell density triggers slender to stumpy
564 differentiation of *Trypanosoma brucei* bloodstream forms in culture. *Mol. Biochem.*
565 *Parasitol.* **90**, 269–280 (1997).
566 14. Vassella, E., Reuner, B., Yutzy, B. & Boshart, M. Differentiation of African trypanosomes is
567 controlled by a density sensing mechanism which signals cell cycle arrest via the cAMP
568 pathway. *J. Cell Sci.* **110 (Pt 2**, 2661–2671 (1997).
569 15. Rico, E. *et al.* Bloodstream form pre-adaptation to the tsetse fly in *Trypanosoma brucei*.
570 *Front. Cell. Infect. Microbiol.* **3**, 78 (2013).
571 16. Vassella, E. *et al.* A major surface glycoprotein of *trypanosoma brucei* is expressed
572 transiently during development and can be regulated post-transcriptionally by glycerol or
573 hypoxia. *Genes Dev.* **14**, 615–626 (2000).
574 17. Naguleswaran, A., Doiron, N. & Roditi, I. RNA-Seq analysis validates the use of culture-
575 derived *Trypanosoma brucei* and provides new markers for mammalian and insect life-
576 cycle stages. *BMC Genomics* **19**, 227 (2018).
577 18. Imhof, S., Knüsel, S., Gunasekera, K., Vu, X. L. & Roditi, I. Social motility of African
578 trypanosomes is a property of a distinct life-cycle stage that occurs early in tsetse fly
579 transmission. *PLoS Pathog.* **10**, e1004493 (2014).
580 19. Oberholzer, M., Lopez, M. A., McLelland, B. T. & Hill, K. L. Social motility in african
581 trypanosomes. *PLoS Pathog.* **6**, e1000739 (2010).
582 20. Eliaz, D. *et al.* Exosome secretion affects social motility in *Trypanosoma brucei*. *PLoS*
583 *Pathog.* **13**, e1006245 (2017).
584 21. DeMarco, S. F., Saada, E. A., Lopez, M. A. & Hill, K. L. Identification of Positive Chemotaxis
585 in the Protozoan Pathogen *Trypanosoma brucei*. *mSphere* **5**, (2020).
586 22. Diaz, E. *et al.* Effect of aliphatic, monocarboxylic, dicarboxylic, heterocyclic and sulphur-
587 containing amino acids on *Leishmania spp.* chemotaxis. *Parasitology* **142**, 1621–1630
588 (2015).
589 23. Pozzo, L. Y. *et al.* Studying taxis in real time using optical tweezers: applications for
590 *Leishmania amazonensis* parasites. *Micron* **40**, 617–620 (2009).
591 24. Barros, V. C., Oliveira, J. S., Melo, M. N. & Gontijo, N. F. *Leishmania amazonensis*:

592 chemotaxic and osmotaxic responses in promastigotes and their probable role in
593 development in the phlebotomine gut. *Exp. Parasitol.* **112**, 152–157 (2006).
594 25. Findlay, R. C. *et al.* High-speed, three-dimensional imaging reveals chemotactic behaviour
595 specific to human-infective Leishmania parasites. *Elife* **10**, (2021).
596 26. Lopez, M. A., Saada, E. A. & Hill, K. L. Insect stage-specific adenylate cyclases regulate
597 social motility in African trypanosomes. *Eukaryot. Cell* **14**, 104–112 (2015).
598 27. Imhof, S., Vu, X. L., Bütikofer, P. & Roditi, I. A Glycosylation Mutant of *Trypanosoma*
599 *brucei* Links Social Motility Defects In Vitro to Impaired Colonization of Tsetse Flies In
600 Vivo. *Eukaryot. Cell* **14**, 588–592 (2015).
601 28. Jelk, J. *et al.* Glycoprotein biosynthesis in a eukaryote lacking the membrane protein Rft1.
602 *J. Biol. Chem.* **288**, 20616–20623 (2013).
603 29. Shaw, S. *et al.* Flagellar cAMP signaling controls trypanosome progression through host
604 tissues. *Nat. Commun.* **10**, (2019).
605 30. Liniger, M. *et al.* Cleavage of trypanosome surface glycoproteins by alkaline trypsin-like
606 enzyme(s) in the midgut of *Glossina morsitans*. *Int. J. Parasitol.* **33**, 1319–1328 (2003).
607 31. Bringaud, F., Ebikeme, C. & Boshart, M. Acetate and succinate production in amoebae,
608 helminths, diplomonads, trichomonads and trypanosomatids: common and diverse
609 metabolic strategies used by parasitic lower eukaryotes. *Parasitology* **137**, 1315–1331
610 (2010).
611 32. Besteiro, S. *et al.* Succinate secreted by *Trypanosoma brucei* is produced by a novel and
612 unique glycosomal enzyme, NADH-dependent fumarate reductase. *J. Biol. Chem.* **277**,
613 38001–38012 (2002).
614 33. Lee, M. G., Bihain, B. E., Russell, D. G., Deckelbaum, R. J. & Van der Ploeg, L. H.
615 Characterization of a cDNA encoding a cysteine-rich cell surface protein located in the
616 flagellar pocket of the protozoan *Trypanosoma brucei*. *Mol. Cell. Biol.* **10**, 4506–4517
617 (1990).
618 34. Affolter, M., Hemphill, A., Roditi, I., Müller, N. & Seebeck, T. The repetitive microtubule-
619 associated proteins MARP-1 and MARP-2 of *Trypanosoma brucei*. *J. Struct. Biol.* **112**,
620 241–251 (1994).

621 35. Ebikeme, C. E. *et al.* N-acetyl D-glucosamine stimulates growth in procyclic forms of
622 *Trypanosoma brucei* by inducing a metabolic shift. *Parasitology* **135**, 585–594 (2008).
623 36. Ruepp, S. *et al.* Survival of *Trypanosoma brucei* in the tsetse fly is enhanced by the
624 expression of specific forms of procyclin. *J. Cell Biol.* **137**, 1369–1379 (1997).
625 37. Zheng, B., Yao, H. & Lee, G. S. Inactivation of the gene encoding the flagellar pocket
626 protein, CRAM, in African trypanosomes. *Mol. Biochem. Parasitol.* **100**, 235–242 (1999).
627 38. Gould, M. K. *et al.* Cyclic AMP effectors in African trypanosomes revealed by genome-
628 scale RNA interference library screening for resistance to the phosphodiesterase
629 inhibitor CpdA. *Antimicrob. Agents Chemother.* **57**, 4882–4893 (2013).
630 39. Shaw, S., Knüsel, S., Hoenner, S. & Roditi, I. A transient CRISPR/Cas9 expression system
631 for genome editing in Trypanosoma brucei. *BMC Res. Notes* **13**, 268 (2020).
632 40. Naguleswaran, A. *et al.* Developmental changes and metabolic reprogramming during
633 establishment of infection and progression of Trypanosoma brucei brucei through its
634 insect host. *PLoS Negl. Trop. Dis.* **15**, e0009504 (2021).
635 41. Saada, E. A. *et al.* Insect stage-specific receptor adenylate cyclases are localized to
636 distinct subdomains of the Trypanosoma brucei Flagellar membrane. *Eukaryot. Cell* **13**,
637 1064–1076 (2014).
638 42. Wright, M. H., Paape, D., Price, H. P., Smith, D. F. & Tate, E. W. Global Profiling and
639 Inhibition of Protein Lipidation in Vector and Host Stages of the Sleeping Sickness
640 Parasite *Trypanosoma brucei*. *ACS Infect. Dis.* **2**, 427–441 (2016).
641 43. Kwon, H., Choi, M., Ahn, Y. & Pak, Y. N-myristoylation regulates insulin-induced
642 phosphorylation and ubiquitination of Caveolin-2 for insulin signaling. *Biochem. Biophys.*
643 *Res. Commun.* (2020) doi:10.1016/j.bbrc.2020.08.072.
644 44. Vélez-Ramírez, D. E. *et al.* APEX2 Proximity Proteomics Resolves Flagellum Subdomains
645 and Identifies Flagellum Tip-Specific Proteins in Trypanosoma brucei. *mSphere* **6**, (2021).
646 45. Rose, C. *et al. Trypanosoma brucei* colonizes the tsetse gut via an immature peritrophic
647 matrix in the proventriculus. *Nat. Microbiol.* **5**, 909–916 (2020).
648 46. Caljon, G. *et al.* The Dermis as a Delivery Site of *Trypanosoma brucei* for Tsetse Flies. *PLoS*
649 *Pathog.* **12**, e1005744 (2016).

650 47. Capewell, P. *et al.* The skin is a significant but overlooked anatomical reservoir for vector-
651 borne African trypanosomes. *Elife* **5**, (2016).
652 48. Trindade, S. *et al. Trypanosoma brucei* Parasites Occupy and Functionally Adapt to the
653 Adipose Tissue in Mice. *Cell Host Microbe* **19**, 837–848 (2016).
654 49. Cremer, J. *et al.* Chemotaxis as a navigation strategy to boost range expansion. *Nature*
655 **575**, 658–663 (2019).
656 50. Le Ray, D., Barry, J. D., Easton, C. & Vickerman, K. First tsetse fly transmission of the
657 'AnTat' serodeme of *Trypanosoma brucei*. *Ann. Soc. Belg. Med. Trop. (1920).* **57**, 369–381
658 (1977).
659 51. Overath, P., Czichos, J. & Haas, C. The effect of citrate/cis-aconitate on oxidative
660 metabolism during transformation of *Trypanosoma brucei*. *Eur. J. Biochem.* **160**, 175–182
661 (1986).
662 52. Brun, R. & Schönenberger. Cultivation and in vitro cloning or procyclic culture forms of
663 *Trypanosoma brucei* in a semi-defined medium. Short communication. *Acta Trop.* **36**,
664 289–292 (1979).
665 53. Lamour, N. *et al.* Proline metabolism in procyclic *Trypanosoma brucei* is down-regulated
666 in the presence of glucose. *J. Biol. Chem.* **280**, 11902–11910 (2005).
667 54. Roditi, I., Carrington, M. & Turner, M. Expression of a polypeptide containing a dipeptide
668 repeat is confined to the insect stage of *Trypanosoma brucei*. *Nature* **325**, 272–274
669 (1987).
670 55. Roditi, I. *et al.* Procyclin gene expression and loss of the variant surface glycoprotein
671 during differentiation of *Trypanosoma brucei*. *J. Cell Biol.* **108**, 737–746 (1989).
672 56. Knüsel, S. & Roditi, I. Insights into the regulation of GPEET procyclin during differentiation
673 from early to late procyclic forms of *Trypanosoma brucei*. *Mol. Biochem. Parasitol.* **191**,
674 66–74 (2013).
675 57. Allemann, N. & Schneider, A. ATP production in isolated mitochondria of procyclic
676 *Trypanosoma brucei*. *Mol. Biochem. Parasitol.* **111**, 87–94 (2000).
677 58. Gadelha, C., Wickstead, B., de Souza, W., Gull, K. & Cunha-e-Silva, N. Cryptic paraflagellar
678 rod in endosymbiont-containing kinetoplastid protozoa. *Eukaryot. Cell* **4**, 516–525 (2005).

679 59. Wheeler, R. J. Use of chiral cell shape to ensure highly directional swimming in
680 trypanosomes. *PLoS Comput. Biol.* **13**, e1005353 (2017).
681 60. Schindelin, J. *et al.* Fiji: An open-source platform for biological-image analysis. *Nat.*
682 *Methods* **9**, 676–682 (2012).
683 61. Florini, F., Naguleswaran, A., Gharib, W. H., Bringaud, F. & Roditi, I. Unexpected diversity
684 in eukaryotic transcription revealed by the retrotransposon hotspot family of
685 *Trypanosoma brucei*. *Nucleic Acids Res.* **47**, 1725–1739 (2019).
686 62. Al Kaabi, A., Traupe, T., Stutz, M., Buchs, N. & Heller, M. Cause or effect of arteriogenesis:
687 compositional alterations of microparticles from CAD patients undergoing external
688 counterpulsation therapy. *PLoS One* **7**, e46822 (2012).
689 63. Beneke, T. *et al.* A CRISPR Cas9 high-throughput genome editing toolkit for
690 kinetoplastids. *R. Soc. open Sci.* **4**, 170095 (2017).
691 64. Furger, A., Schürch, N., Kurath, U. & Roditi, I. Elements in the 3' untranslated region of
692 procyclin mRNA regulate expression in insect forms of Trypanosoma brucei by
693 modulating RNA stability and translation. *Mol. Cell. Biol.* **17**, 4372–4380 (1997).
694 65. Furger, A., Jungi, T. W., Salomone, J. Y., Weynants, V. & Roditi, I. Stable expression of
695 biologically active recombinant bovine interleukin-4 in Trypanosoma brucei. *FEBS Lett.*
696 **508**, 90–94 (2001).
697 66. Burkard, G., Fragoso, C. M. & Roditi, I. Highly efficient stable transformation of
698 bloodstream forms of *Trypanosoma brucei*. *Mol. Biochem. Parasitol.* **153**, 220–223
699 (2007).
700 67. Schumann Burkard, G., Jutzi, P. & Roditi, I. Genome-wide RNAi screens in bloodstream
701 form trypanosomes identify drug transporters. *Mol. Biochem. Parasitol.* **175**, 91–94
702 (2011).
703

704 **Acknowledgements**

705 Berta Pozzi, Stephanie DeMarco and Boris Striepen are thanked for stimulating discussions and
706 constructive comments on the manuscript. We are indebted to Jan van den Abbeele, Institute
707 of Tropical Medicine, Antwerp for a gift of tsetse pupae.

708 This research was supported by the Swiss National Science Foundation (Grant numbers
709 310030_184669 and 31003A_166427) and the Canton of Bern.

710 **Author contributions**

711 S.S., S.K., A.N., D.A. and I.R. conceived, designed and conducted experiments. R.E. and M.B.
712 conducted experiments. S.S., S.K., A.N., D.A., R.E. and I.R. analysed the data. S.S. and I.R. wrote
713 the paper.

714 **Figure Legends**

715 **Fig. 1** Response of migrating cells to fresh medium (DTM) and conditioned medium (CM) after
716 different treatments. **a** Upper panel: communities exposed to DTM and CM; lower left panel:
717 communities exposed to filtered CM on both sides; lower right panel: communities exposed to
718 dialysed CM (12 kDa cut-off) or undialysed CM. White circles with dots indicate where solutions
719 were pipetted onto the plates. Community lifts stained for EP (green) and GPEET (red) are shown.
720 **b** Continuous growth in liquid culture acidifies medium. Representative pictures of culture
721 supernatants from early procyclic forms (EATRO1125) grown in DTM for 7 days without dilution.
722 Left, DTM only. Samples were taken on days 0, 4 and 7. The colour change from red to yellow
723 indicates that the culture becomes more acidic with time. Cell titres are indicated.
724
725 **Fig. 2** Trypanosomes acidify their environment in liquid culture and on semi-solid agarose plates**.**
726 Early procyclic forms (Lister 427 Bern) grown in SDM79 were analysed. **a** pH (left y axis) of
727 medium only, a log-phase culture (log, 3.9 x 10^6 cells ml^{-1}) and a dense culture (dense, 5.6 x 10^7
728 cells ml^{-1}). Three technical replicates are shown. The H^+ concentration is indicated on the right y
729 axis. Medium only was incubated for the same length of time as the cultures. **b** and **c** pH
730 measurements on SoMo plates. **b** Trypanosomes (2 x 10^5 cells) were either spotted onto the
731 centre of a plate as a single inoculum (left row) or in pairs (right row). White numbers indicate
732 pH measurements on days 0, 2, 3, 4 and 7 in the centre of a community, at the periphery and in
733 the space between two communities (indicated with a white arrow). **c** Graphs for pH
734 measurement shown in **b**. Each data point represents the mean pH measured from replicate
735 plates, error bars depict the range (n=2). Top: plates with single communities. pH at the plate

736 periphery (○ dashed line) or in the centre of the community (● solid line). Bottom: paired
737 communities. pH at the plate periphery (○ dashed line), in the centres of the two communities
738 (▼ or ▲ solid line), or between them (◆ dotted line). Y axes are the same as in **a.**
739 **d** The time-point of migration depends on the volume of the substrate. Equal numbers of early
740 procyclic forms were inoculated onto wells that contained different volumes of medium with
741 agarose. Plates were photographed on days 3, 4 and 5 post inoculation.
742
743 **Fig. 3** Response of early and late procyclic forms to acidic or basic solutions. **a** Schematic
744 representation of the pH taxis assay. "x" represents the site where a solution was spotted. "D" is
745 the distance between the closest projection and the spot. In these experiments D= 1.3 cm. **b** Early
746 procyclic forms (EATRO1125) on DTM plates were exposed to NaOH (OH- treatment) or HCl (H+
747 treatment) on both sides of the population. **c** Late procyclic forms were exposed to NaOH on the
748 right side and HCl on the left side of the community. Scale bar: 1 cm. For **b** and **c** community lifts
749 stained for EP (green) and GPEET (red) are shown.
750
751 **Fig. 4** Volcano plots comparing transcriptomes of cells from different regions of a community or
752 following exposure to acid or alkali. DTM plates were inoculated with cells from liquid cultures of
753 early procyclic forms (EATRO1125) in DTM medium. **a** Comparison of the roots and tips of
754 projections. For clarity the same volcano plot is displayed twice with different transcripts
755 annotated. Left: early procyclic form markers, such as GPEET, calflagin, hexokinase 1 and
756 prostaglandin F synthetase are upregulated in tips. Adenylate cyclases such as ACP3, ACP5 and
757 ACP6 are differentially expressed between tip and root. Right: glycolytic enzymes and genes
758 involved in glucose metabolism are upregulated in tips. Far-right panel: community lift of a
759 representative SoMo plate 7 days after inoculation stained for EP (green) and GPEET (red). Tips
760 were isolated when projections were ≥ 2.5 cm in length. RNA-seq was performed in duplicate. **b**
761 Pairwise comparisons of untreated communities and communities exposed to acid or alkali. Tips
762 were isolated from projections showing a clear response to the treatment (indicated with red
763 circles). RNA-seq was performed in triplicate. The illustrations in the left and right bottom corners
764 of the volcano plots show SoMo communities (in black) and the samples that were collected (red
765 circles).

766

767 **Fig. 5** Glucose availability impacts SoMo by acidification of the culture medium. Procyclic forms
768 (Lister 427 Bern) grown in SDM79 or SDM80 plus supplements were analysed: SDM79 (blue / ○),
769 SDM80+G6 (+ 6 mM glucose, green / □), SDM80+N6 (+ 6 mM GlcNAc, red / △). If not specified,
770 cells were adapted from SDM79 to the medium indicated for one to three weeks. **a** Social motility
771 on semi-solid plates was assessed in SDM80 with varying glucose availability. Left: SoMo plates
772 on day 6 after inoculation, prior to performing community lifts. Cells were adapted from
773 SDM80+G6 to the corresponding liquid medium for 5 days before inoculation. Right: merge of
774 the corresponding community lifts probed for GPEET (red) and EP (green). **b** Flow cytometric
775 analysis. The percentage of GPEET-positive cells (shaded area) is indicated. Cells grown in SDM79
776 were used as a control (2° antibody only, grey). **c** Cumulative growth in different media. Growth
777 was monitored after transferring cells from SDM79 to the corresponding medium 3 days earlier.
778 Numbers indicate population doubling time averaged over 7 days (mean ± SD). **d** Steady-state
779 ATP levels in different media. Cell lysates were harvested in two independent experiments
780 (replicate 1 or 2, respectively). Cell densities at harvest were between 6.2 - 8.0 or 7.3 - 8.9 x 10^6
781 cells ml^{-1}, respectively. Appropriate dilutions of cell lysates were assayed; the graph depicts
782 means and error bars (SD) of technical replicates shown as circles (n=12 or 9, respectively). Data
783 are shown relative to SDM80+G6. **e** Directional motility in different media. Cell densities at
784 harvest were between 5.9 - 6.5 x 10^6 cells ml^{-1}. Centred motility tracks of individual cells are
785 shown at identical scale. > 6000 tracks in each medium were pooled from nine movies acquired
786 from three technical replicates.
787 **f** pH measurement of liquid cultures. Culture medium (medium only) and supernatants from log-
788 phase (log) or dense culture (dense). Cell titres per ml in SDM79, SDM80+G6 or SDM80+N6,
789 respectively: 3.2 x 10^6, 3.8 x 10^6 or 3.3 x 10^6 (log) and 5.1x 10^7, 4 x 10^7or 3.6 x 10^7 (dense). Three
790 technical replicates are shown for each condition. The corresponding H^+ concentration is
791 indicated on right y axis. **g** pH measurements on SoMo plates inoculated with cells pre-adapted
792 to the corresponding liquid medium. ΔpH (centre − periphery) refers to pH in centre of the
793 community minus the pH at the plate periphery. Each data point represents the mean ΔpH from
794 replicate plates, error bars depict the range (n=3). The fold change in H^+ concentration is
795 indicated on the right y axis.

796

797 **Fig. 6** CARP3 is required for acid sensing in vitro and for establishment of infection in flies.
798 **a** Merged EP and GPEET signals of Lister 427 wt and PDEB1 knockout (KO). **b** Merged EP and
799 GPEET signals of 427 Cas9 parental line, CARP3 knockout and CARP3-HA addback. Upper panel:
800 untreated. Lower panel: exposed to acid and alkali. **c** Teneral flies were infected with wild-type
801 Lister 427 procyclic forms (WT), the CARP3 double knockout (CARP3-KO) and the addback (AB).
802 Dissections were performed 13-14 days post infection. Total numbers are derived from two
803 replicates per cell line (Supplementary Table 3). The intensity of midgut infections was scored as
804 heavy, intermediate or weak as described[36]. The p-value is shown for Fisher's exact test, two-
805 sided. **d** Western blot analysis of immunoprecipitations with anti-HA and anti-myc antibodies
806 (representative blot from three independent experiments). Myc-tagged ACP3 and ACP5 were
807 expressed independently in the CARP3-HA background. The parental line 427 Cas9 was used as a
808 control. Input samples have 40 times fewer cell equivalents than the immunoprecipitated
809 samples. IP: immunoprecipitation with anti-HA or anti-myc antibodies. **e** Merged EP and GPEET
810 signals of the 427 Cas9 parental line and 3 independent ACP5 single allele knockouts; panels as
811 in **b**. **f** Myc-tagged ACP5 is localised to the flagellar tip in a cell line co-expressing CARP3-HA.
812 Immunofluorescence was performed with an anti-myc antibody (red). DNA was stained with
813 Hoechst dye. Scale bar = 10 µm. **g** Summary of mutants, SoMo phenotypes and responses to pH.
814 -/-: double knockouts; +/-: single knockouts.

815

816 **Supplementary Fig. 1** Different chemicals were tested for their impact on migrating cells on semi-
817 solid surfaces. Procyclic forms of EATRO1125 were incubated on DTM plates. **a** All chemicals
818 were dissolved or diluted in water to give 1 M solutions. Chemicals highlighted in red could not
819 be dissolved completely, but were used anyway. **b** Effect on migrating cells and pH of 1M
820 solutions. **c** SoMo assays. Chemicals were spotted on day 4 after inoculation and photographs
821 were taken 16-20 h later. Photographs were processed to improve contrast and converted to
822 black and white.

823

824 **Supplementary Fig. 2** Independent CRAM knockout clones exposed to acid and alkali. **a** Upper
825 panel: community lifts of CRAM knockout clones and their 427 Cas9 parental cell line. Lower

826 panel: community lifts of knockouts and the parental line exposed to acid (H^+) and alkali (OH^-).
827 The images show merged EP and GPEET signals. **b** Growth comparison of three individual CRAM
828 knockouts and parental 427 Cas9.
829
830 **Supplementary Fig. 3** Characterisation of CARP3 and CARP4 knockouts. **a** Genotyping of CARP3
831 and CARP4 knockouts by PCR. Genomic DNA was isolated from individual clones and amplified
832 with the primers listed in Supplementary Table 5. **b** Community lifts of two individual CARP4
833 knockout clones. **c** Growth comparison of CARP3 and CARP4 knockouts and parental 427 Cas9. **d**
834 Determination of cell numbers on plates. Starting with an inoculum of 2 x 10^5 cells, cell numbers
835 were determined for 427 Cas9, the CARP3 knockout and the HA-tagged addback on days shown
836 in the figure. Cells were harvested by flushing the surface of the plate with PBS and cell numbers
837 were determined using a haemocytometer. Cells from all three lines were observed to giggle
838 under the microscope **e** Percentage of GPEET-positive cells (shaded area) is indicated. Cells
839 without prior incubation with anti-GPEET antiserum were used as a negative control (2° antibody
840 only, grey).
841
842 **Supplementary Fig. 4** Motility and localization studies of CARP3 knockout. **a** Motility assay of
843 CARP3 knockouts. Centred motility tracks of individual cells are shown at identical scale. > 8000
844 tracks for each cell line (427 Cas9, CARP3 KO Cl.1, CARP3 KO Cl.2 and Trypanin KO, respectively)
845 were pooled from nine movies acquired from three technical replicates. The trypanin knockout
846 was used as a motility-deficient control[29]. **b** Velocity and speed of each cell line. The colour code
847 corresponds to the cell lines in d. Data points are displayed as box plot with whiskers representing
848 2.5 - 97.5 percentile, filled circles represent points outside that range. InterQuartileRange IQR
849 (25 - 75 percentile), with Median (50 percentile). **c** Localisation of CARP3-HA (green) by
850 immunofluorescence. DNA was stained with Hoechst dye. Scale bar = 10 µm.
851
852 **Supplementary Fig. 5** Genotyping of the CARP3 knockout (**a**) and addback (**b**) used for the fly
853 experiments.
854

855 **Supplementary Fig. 6** Characterisation of ACP knockouts. **a** Genotyping of ACP knockouts by PCR.
856 Genomic DNA was isolated and PCRs were performed with the primers listed in Supplementary
857 Table 5. **b** SoMo and pH taxis assays. Plates were inoculated with the cell lines indicated and 4
858 days later HCl and NaOH were applied to the plates (indicated by dots). Pictures were taken 16-
859 20 h after spotting of chemicals. **c** Growth of ACP5 single knockout clones compared to the
860 parental 427 Cas9 cell line. **d** Motility assays of ACP5 single knockouts. Centred motility tracks of
861 individual cells are shown at identical scale. > 7000 tracks for each clone were pooled from nine
862 movies acquired from three technical replicates. The parental line 427 Cas9 and Trypanin KO
863 were used as controls. **e** Velocity and speed of individual cell lines. The colour code corresponds
864 to the cell lines in d. Data points are displayed as box plot with whiskers representing 2.5 - 97.5
865 percentile, filled circles represent points outside that range. InterQuartileRange IQR (25 - 75
866 percentile), with Median (50 percentile). **f** Flow cytometric analysis of percentages of GPEET-
867 positive cells.
868
869 **Supplementary Table 1** RNA-seq data. **a** Comparison of the roots and tips of projections.
870 Transcripts from the tips either upregulated >1 Log2FC or downregulated <1 Log2FC in
871 comparison to the root. FC: fold change. **b** Pairwise comparisons of untreated communities and
872 communities exposed to acid or alkali. Transcripts from tips that were either upregulated >1
873 Log2FC or downregulated <1 Log2FC. FC: fold change. Raw read files are deposited at the
874 European Nucleotide Archives (ENA) http://www.ebi.ac.uk/ena as study PRJEB41935.
875
876 **Supplementary Table 2** Measurements of distances migrated by 427 WT and PDEB1 knockout
877 parasites after exposure to acid and alkali. Parasites were inoculated as described for SoMo
878 assays and incubated for four days. 1M HCl and NaOH (30 µl each) were added to the plates at
879 a distance of 1.5 cm from the edge of the community for the PDEB1 knockout and from the tips
880 of the protrusions for 427 WT (Fig. 3a, D = distance). The plates were sealed with parafilm and
881 incubated at 27 °C for 16-20 hours. Positive numbers are migration towards and negative
882 numbers are migration away from the spotted acid or alkali. Standard deviations were
883 calculated from 5 samples each.
884

885 **Supplementary Table 3** Fly infections. Midgut and proventriculus infection rates from two
886 independent experiments with 427 Cas9, the CARP3 knockout and the untagged CARP3
887 addback.
888
889 **Supplementary Table 4** Proteins interacting with CARP3-HA, ACP3-Myc and ACP5-Myc
890 identified by liquid chromatography – mass spectrometry (LC-MS).
891
892 **Supplementary Table 5** List of primers used for knockouts and genotyping.
893
894 **Supplementary Video 1** Early procyclic form parasites exhibit social motility.
895
896 **Supplementary Video 2** Response of early procyclic forms to hydrochloric acid (HCl). Black arrows
897 indicate where solutions were spotted. The video is shown as a rewind loop.
898
899 **Supplementary Video 3** Response of early procyclic forms to sodium hydroxide (NaOH). Black
900 arrows indicate where solutions were spotted. The video is shown as a rewind loop.
901
902 **Supplementary Video 4** Response of late procyclic forms to sodium hydroxide (NaOH). Black
903 arrows indicate where solutions were spotted. The video is shown as a rewind loop.

Figure 1

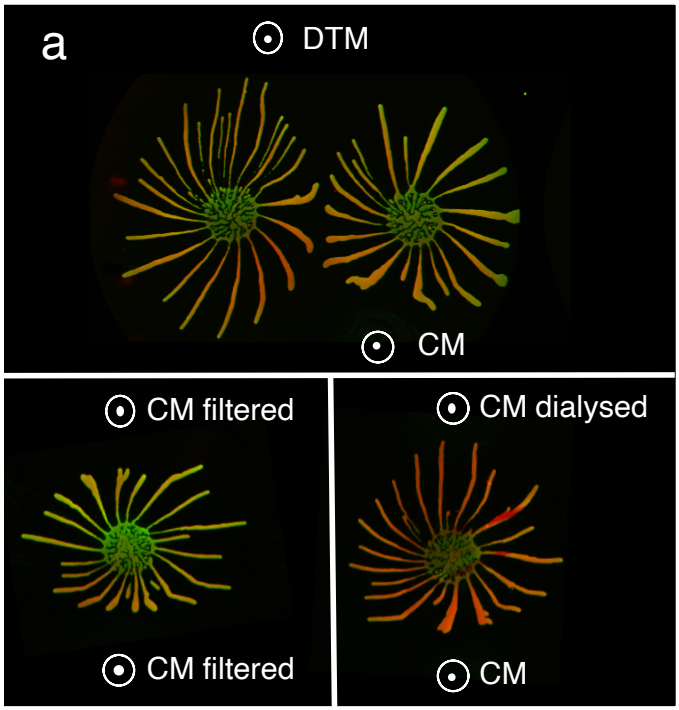
a
DTM
CM
CM filtered
CM filtered
CM dialysed
CM

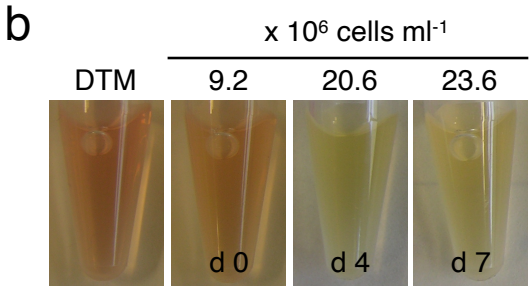
b
x 10⁶ cells ml⁻¹
DTM
9.2
20.6
23.6
d 0
d 4
d 7

Figure 2

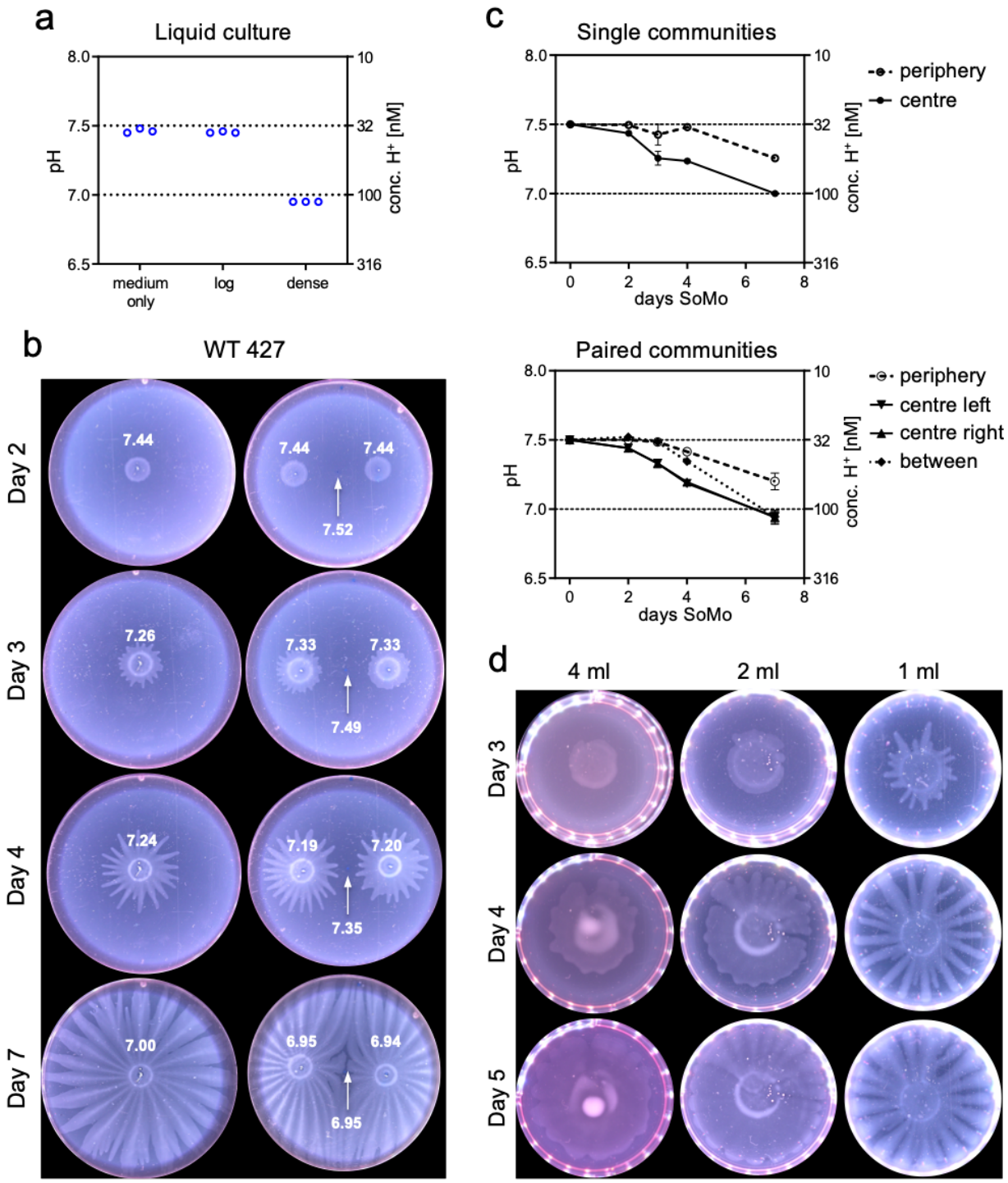
a
Liquid culture
pH
conc. H+ [nM]
8.0
7.5
7.0
6.5
10
32
100
316
medium only
log
dense
b
WT 427
Day 2
Day 3
Day 4
Day 7
7.44
7.44
7.44
7.52
7.26
7.33
7.33
7.49
7.24
7.19
7.20
7.35
7.00
6.95
6.94
6.95
c
Single communities
Paired communities
days SoMo
periphery
centre
centre left
centre right
between
d
4 ml
2 ml
1 ml
Day 3
Day 4
Day 5

Figure 3

a

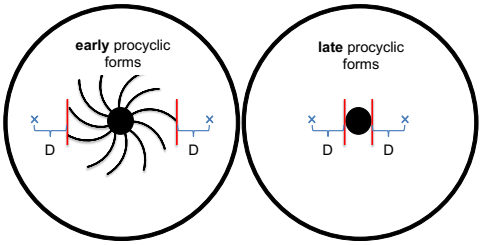
early procyclic forms
D
D
late procyclic forms
D
D

b

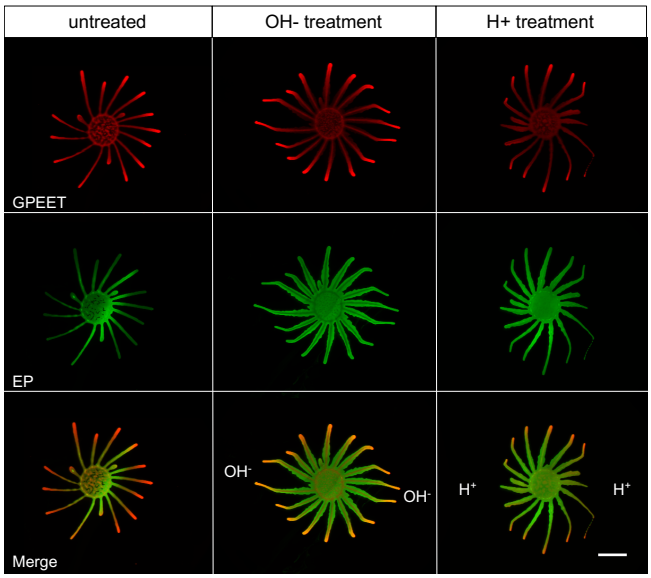
untreated
OH- treatment
H+ treatment
GPEET
EP
Merge
OH-
OH-
H+
H+

c

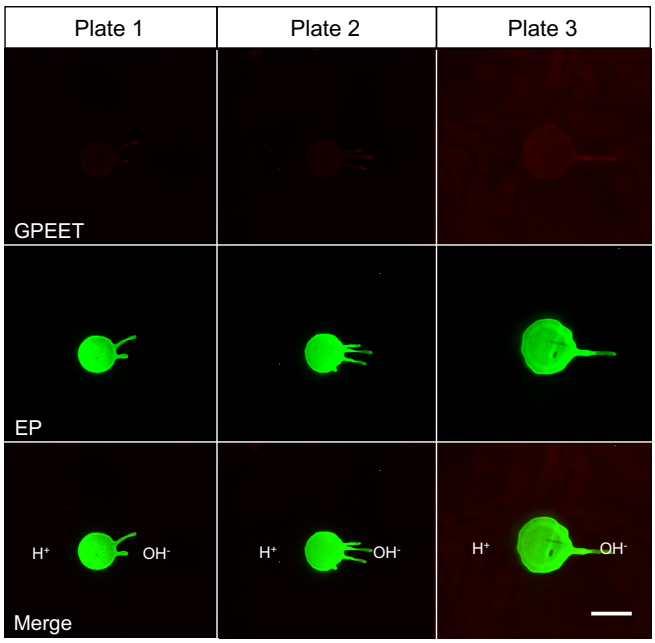
Plate 1
Plate 2
Plate 3
GPEET
EP
Merge
H+
OH-
H+
OH-
H+
OH-

Figure 4

a

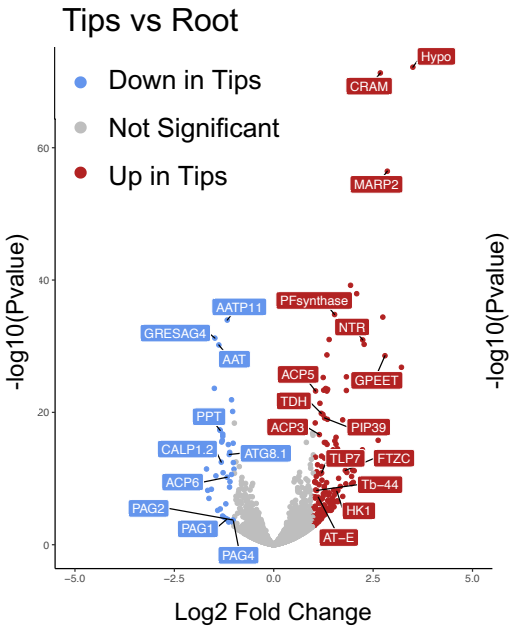
Tips vs Root
Down in Tips
Not Significant
Up in Tips
-log10(Pvalue)
Log2 Fold Change
Hypo
CRAM
MARP2
PFsynthase
NTR
GPEET
ACP5
TDH
ACP3
PIP39
TLP7
FTZC
Tb–44
HK1
AT–E
AATP11
GRESAG4
AAT
PPT
CALP1.2
ATG8.1
ACP6
PAG2
PAG1
PAG4

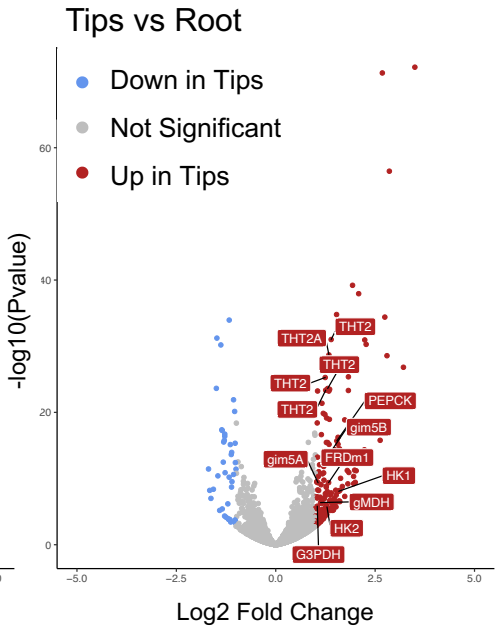
Tips vs Root
Down in Tips
Not Significant
Up in Tips
-log10(Pvalue)
Log2 Fold Change
THT2A
THT2
THT2
THT2
THT2
PEPCK
gim5B
gim5A
FRDm1
HK1
gMDH
HK2
G3PDH

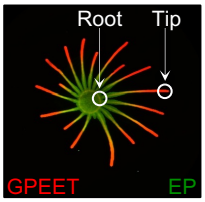
Root
Tip
GPEET
EP

b

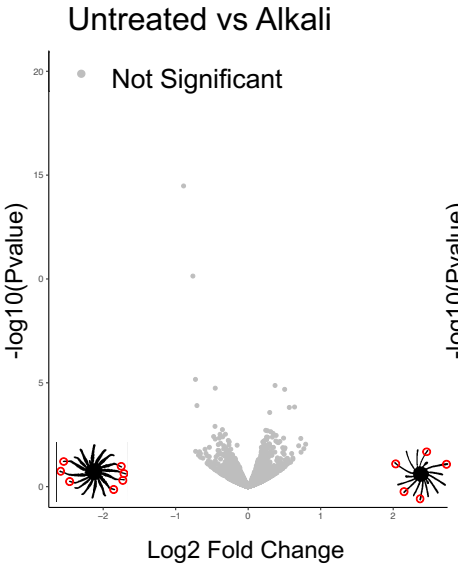
Untreated vs Alkali
Not Significant
-log10(Pvalue)
Log2 Fold Change

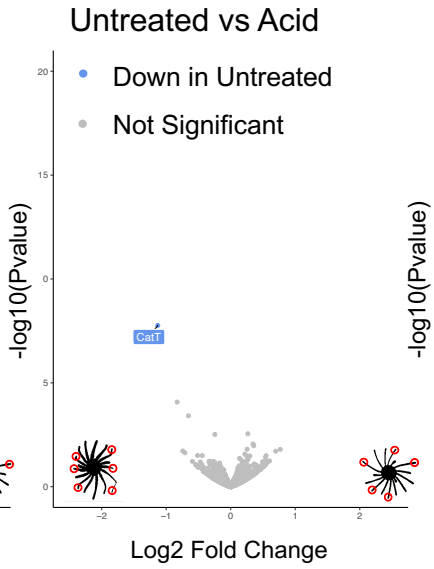
Untreated vs Acid
Down in Untreated
Not Significant
CatT
-log10(Pvalue)
Log2 Fold Change

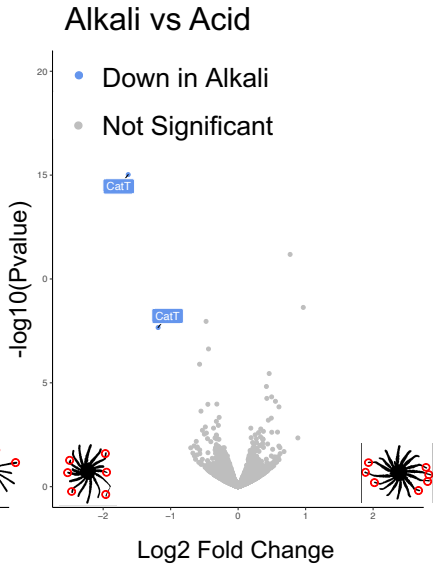
Alkali vs Acid
Down in Alkali
Not Significant
CatT
CatT
-log10(Pvalue)
Log2 Fold Change

Figure 5

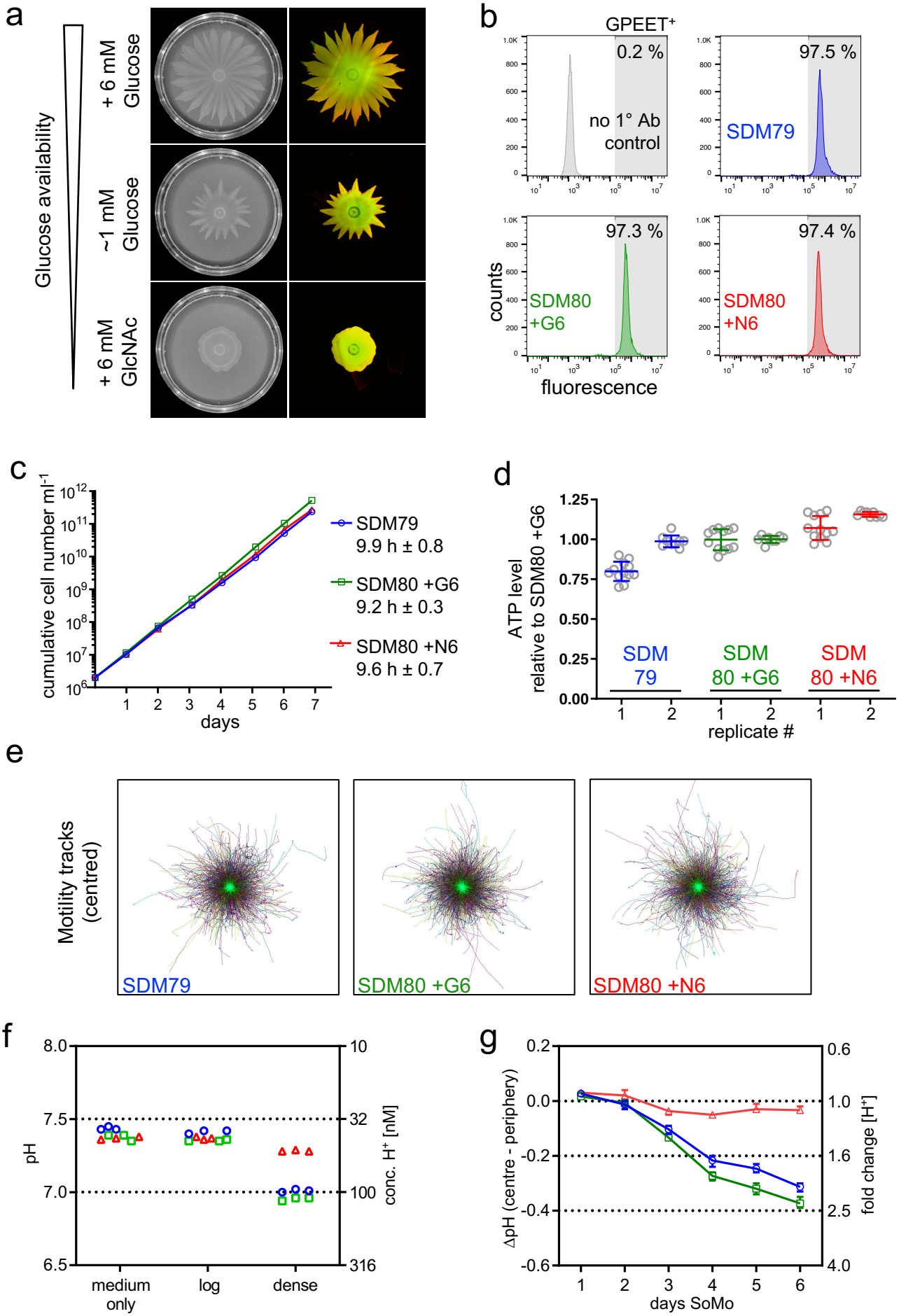
a
Glucose availability
+ 6 mM Glucose
~1 mM Glucose
+ 6 mM GlcNAc
b
GPEET+
0.2 %
no 1° Ab control
97.5 %
SDM79
97.3 %
SDM80 +G6
97.4 %
SDM80 +N6
counts
fluorescence
c
cumulative cell number ml-1
days
SDM79
9.9 h ± 0.8
SDM80 +G6
9.2 h ± 0.3
SDM80 +N6
9.6 h ± 0.7
d
ATP level relative to SDM80 +G6
SDM 79
SDM 80 +G6
SDM 80 +N6
replicate #
e
Motility tracks (centred)
SDM79
SDM80 +G6
SDM80 +N6
f
pH
conc. H+ [nM]
medium only
log
dense
g
ΔpH (centre - periphery)
fold change [H+]
days SoMo

Figure 6

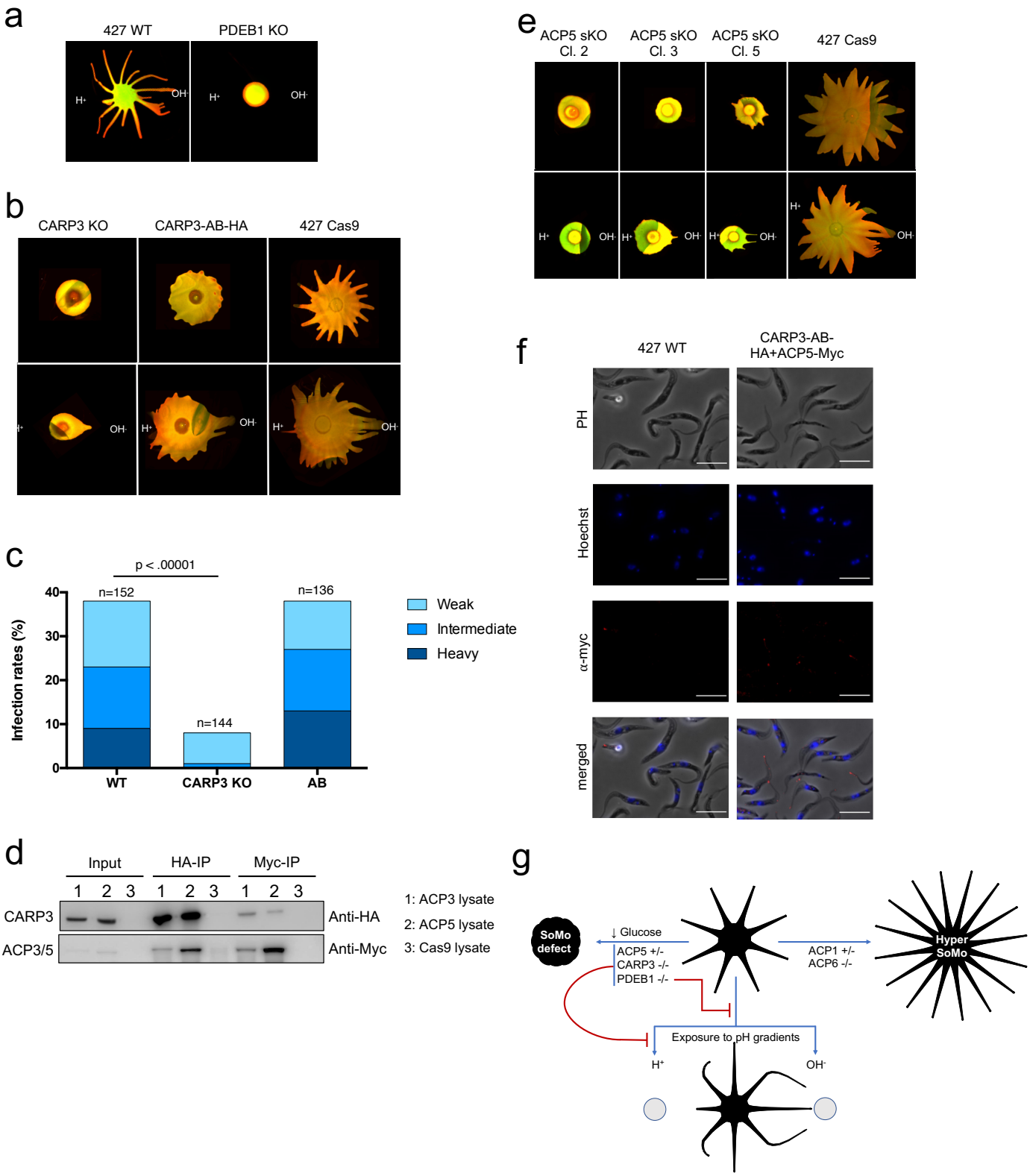
a
427 WT
PDEB1 KO
H+
OH-
b
CARP3 KO
CARP3-AB-HA
427 Cas9
c
p < .00001
n=152
n=144
n=136
Infection rates (%)
WT
CARP3 KO
AB
Weak
Intermediate
Heavy
d
Input
HA-IP
Myc-IP
1 2 3 1 2 3 1 2 3
CARP3
ACP3/5
Anti-HA
Anti-Myc
1: ACP3 lysate
2: ACP5 lysate
3: Cas9 lysate
e
ACP5 sKO Cl. 2
ACP5 sKO Cl. 3
ACP5 sKO Cl. 5
427 Cas9
f
427 WT
CARP3-AB-HA+ACP5-Myc
PH
Hoechst
α-myc
merged
g
SoMo defect
↓ Glucose
ACP5 +/-
CARP3 -/-
PDEB1 -/-
ACP1 +/-
ACP6 -/-
Hyper SoMo
Exposure to pH gradients
H+
OH-